Magnetic anisotropy of plastically deformed low-carbon steel

O Stupakov, T Uchimoto, T Takagi

Magnetic anisotropy of plastically deformed low-carbon steel

O Stupakov[1], T Uchimoto[2] and T Takagi[2]

E-mail: `stupak@fzu.cz`, URL: `www.fzu.cz/~stupak`
[1]Institute of Physics of the AS CR, v.v.i., Na Slovance 2, 18221 Prague, Czech Republic
[2]Institute of Fluid Science, Tohoku University, Katahira 2-1-1, Aoba-ku, Sendai 980-8577, Japan

Abstract. Macroscopic hysteresis and local Barkhausen noise techniques were used for the comprehensive magnetic investigation of structural low-carbon steel subjected to uniaxial plastic tension. Scattering of the measured magnetic parameters was substantial within the Lüders band region with stabilization at higher strains. Compressive residual stresses in the deformation direction formed a hard magnetization axis with intriguing two-phase remagnetization. The magnetic parameters had highest sensitivity to strain in this direction. They changed as $\cos^2$ with rotation to the perpendicular easy magnetization axis, where the magnetic sensitivity was lowest. The relation between the deformed steel microstructure (dislocation and residual stress patterns) and the obtained magnetic behaviour is interpreted. Applicability of the examined techniques for the non-destructive characterization of steel degradation is discussed.

PACS numbers: 75.60.Ej, 75.80.+q, 75.50.Bb, 62.20.F, 81.70.Ex

Submitted to: *J. Phys. D: Appl. Phys.*

1. Introduction

The magnetic response of construction ferromagnetic materials to the plastic deformation has been investigated for about 150 years [1, 2]. However, recent results obtained using modern measurement techniques have stimulated further research. Interesting features of deformed ferromagnetic materials as two-phase remagnetization and coincident hysteresis points were ascribed to magnetoelastic coupling with residual stress and not to the domain wall (DW) pinning on accumulated dislocations, as previously believed [3, 4, 5, 6]. However, the important topic of magnetic anisotropy caused by uniaxial deformations has been little investigated so far, probably owing to the difficulties of realizing such experiments [4, 6, 7, 8].

Aside from its scientific interest, the problem is topical in terms of industrial application. At present, there is a strong demand for the non-destructive reliable estimation of the remaining lifetimes of steel constructions; e.g., constructions in power plants [9]. The present work was conducted in the framework of round robin testing organized by Tokyo Electric Power Company. Their interest was stimulated by a large earthquake near Niigata in 2007, when an atomic power plant was taken out of service for a long period. Among other non-destructive testing methods, the considered magnetic techniques were examined and found to have good potential for the characterization of mechanical degradations of construction steels.

Comparing with previous works [3, 4, 6, 8], including our own [5, 7, 9], the present work proposes more accurate and detailed measurements of the magnetic anisotropy with direct field control, good result statistics, and simultaneous investigations of the macroscopic bulk hysteresis and the local sub-surface Barkhausen noise (BN) magnetic responses [10]. An initial region of plastic deformation, characterized by inhomogeneous dislocation (Lüders bands) and residual stress patterns, was investigated in detail [11, 12]. On the basis of the data obtained, our previous experience and other published results, the observed magnetic behaviour was explained in terms of the magnetoelastic coupling with the applied/residual stresses and the DW pinning on accumulated dislocations. The general question of the influence of the steel microstructure on the magnetic properties was also discussed.

2. Experimental details

Measurements were made for a low-carbon steel SS400 (0.1–0.12% C, 0.58% Mn, 0.21% Si, max. 0.013% P, max. 0.014% S) used for large-diameter pipelines in Japanese power plants. This rolled steel was specially designed to enhance seismic safety of building structures (yield point $\geq$ 245, typically 390 MPa; tensile strength is 400–510, typically 480 MPa; elongation $\geq$ 21, typically 38%). The microstructure is composed of ferrite and pearlite with the phase ratio of $\sim 9/1$ (see figure 1). The polyhedron ferrite grains of ~ 10 μm size do not display the signs of mechanical working; this structure corresponds to the state after normalizing annealing.

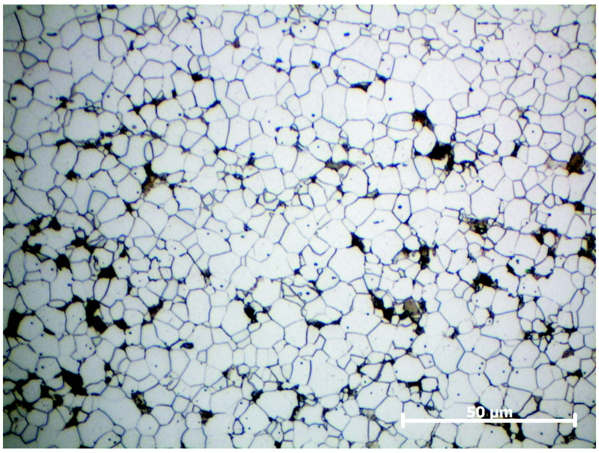

Figure 1. Optical microscope image of the SS400 steel at 1000 magnification.

The steel was purchased from two different producers as 500x100x3 mm^3 sheets with the longest sides being along the rolling direction. Three identical sheets from the first producer were stretched in the rolling direction to obtain target residual strains of about 0, 0.2, 0.5, 1, 2, 5, and 10% (first series of 21 samples). Two identical sheets from the second producer were stretched similarly to obtain strains of 0, 0.2, 0.5, 1, 2, 5, 10, 15, and 20% (second series of 18 samples). Six strain gauges were mounted along the stress direction on both sides of the samples to control the real deformation conditions. The stress-strain curves were typical for iron-based low-carbon steel with a wide region of plastic instability (hereafter the Lüders band region) from 0.15–0.2% to 3.5–5% strain [11, 13].

For the measurements, samples with dimensions of 70x70x3 mm^3 were mechanically cut from the centers of the deformed sheets without appreciable heating of the sample edges. Readings of the strain gauges, placed at the center of the samples on both sides, were used for the result presentation. They were accurately removed before the magnetic measurements. The gauges recorded substantial data scattering in the Lüders band range [12]. Therefore, the samples were measured not only parallel and perpendicular to the applied stress, but also on both sample sides. For a detailed investigation of the magnetic anisotropy, four samples of the first series strained at 0, 1, 5, and 10% were machined to discs of 60 mm diameter to avoid shape-induced measurement error [6, 14]. These experiments were performed for both disc sides with the magnetization line rotating through a 180^o range in 20^o steps.

The magnetic measurements were conducted using a homemade setup described in detail in reference [15]. The magnetically open samples were magnetized by a single Fe-Si yoke of 70 mm width with inner and outer pole distances of 40 and 90 mm. The magnetization coil placed on the yoke was governed by a triangular voltage waveform with a frequency of 0.2 Hz (near quasi-static magnetization regime for the hysteresis measurements). The sample magnetization was controlled by a sample-wrapping induction coil and a vertical array of three Hall sensors. This array measured the surface field profile above the samples, which was linearly extrapolated to the specimen face to determine the real sample field [16]. The measurements were performed with maximum magnetic flux density of 1.7 T for the square plate samples and 1.35 T for the discs, which were assumed to be magnetized homogeneously [14]. BN was detected by a surface-mounted pancake coil of 1000 turns with 15 mm outer diameter, inserted in a grounded Cu shielding case. Its laminated soft magnetic Fe-Si core with dimensions of 4x4x14 mm^3 was gently weighted by a spring to ensure good contact with the sample face. The BN signal was sampled at 500 kHz and filtered in a 2–50 kHz bandwidth (the resonance frequency of BN sensor was 130 kHz). The Hall array and BN coil were placed at the center of the yoke-free sample side, exactly where the strain gauges were mounted. The magnetic responses were studied in great detail; various magnetic parameters were evaluated against the directly measured field, residual strain and magnetization angle.

3. Results

Similar results were obtained for the two sample series, the only difference being that the first series had slightly higher scatter in the strain gauge reading and magnetic measurement data in the Lüders band region. Therefore, for the sake of simplicity, most of the results are illustrated for the second series with a larger strain span by default.

Along the direction of stress the magnetization proceeds in two stages, which is well seen in the two-peak profiles of the differential permeability and the BN envelopes [5, 6]. This leads to a bulging of the hysteresis loops, which additionally rotate around the coincident intersection points in the second and the fourth quadrants with the strain (see figure 2(a); for the sake of simplicity, only the ascending hysteresis branches are shown) [2, 17]. Thereby the magnetic properties significantly deteriorate as illustrated by the dependence of the classical coercive force on the residual strain (see figure 2(b)). All magnetic parameters have large scattering in the Lüders band region, where the sample microstructure is not settled. The coercivity data are fitted by a theoretically predicted power law $H_c \sim \varepsilon_r^{0.3-0.5}$ [18]. Other classical hysteresis parameters behave similarly; the losses increase and the remanence and maximum differential permeability decrease [5, 19]. Therefore, *the direction perpendicular to the deformation* with lower compressive and higher tensile residual stresses becomes the easy magnetization axis [7, 12]. The hysteresis loops measured in the perpendicular direction are of usual rectangular shape with similar but much less pronounced rotation around the coincident points (figure 2(a)) [6]. The hysteresis parameters have similar but much less sensitive dependencies on the strain as compared with the stress direction (figure 2(b)).

The BN envelopes for different strains are shown in figure 3(a). The deformed samples demonstrate clear two-phase magnetization in the stress direction and a BN increase in the perpendicular direction; i.e., along the easy magnetization axis [4, 7]. The time integrals of envelope voltage as functions of magnetic field (BN loops) appear

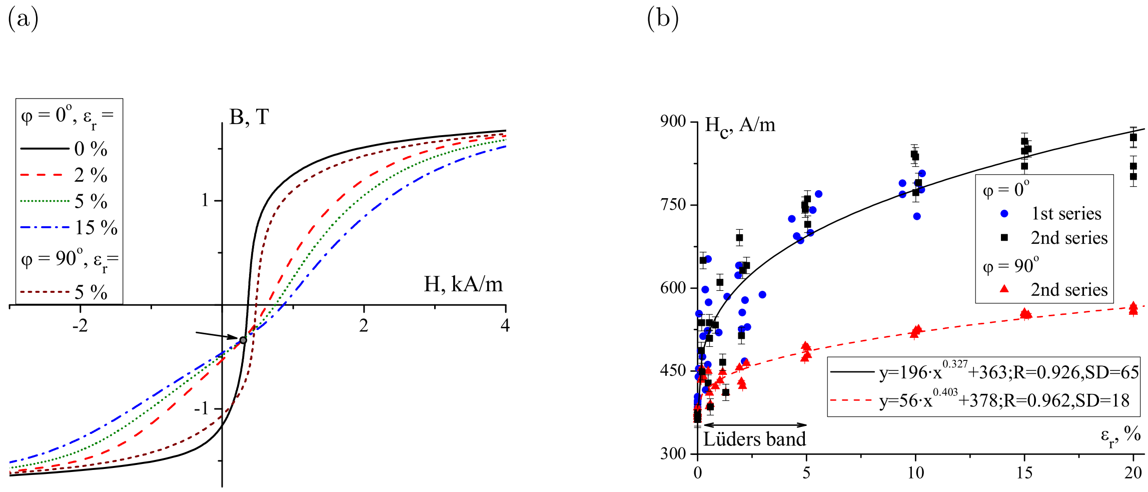

Figure 2. (a) Ascending hysteresis branches for different residual strains and magnetization angles ($\varphi = 0^o$ is the stress direction). The coincident point is indicated by the arrow. (b) Coercive force H_c versus residual strain parallel and perpendicular to the stress. The error bars present the standard error, estimated from the data deviation beyond the Lüders band region. The dependencies are fitted by a theoretically predicted power law. The Pearson correlation coefficient R and standard deviation of the fit SD are given in the graph label.

similar to the hysteresis loops; however, they are not normalized in Y-axis. The most useful and stable parameter, which can be obtained from the BN loop, seems to be BN coercivity, which is introduced similarly to its hysteresis analogue (see figure 3(b)) [15]. As shown in figure 4, BN coercivity has good linear correlation with the real coercive force up to high strains in the stress direction. The dependencies of the classical root mean square (RMS) value of BN on strain are shown in figure 5(a). The figure shows a monotonous steep increase within the Lüders band region in the perpendicular direction, but larger scatter of the results. In the stress direction, the RMS value has a near-linear decay after a rapid initial increase [4, 5, 7]. On the basis of the specific two-peak magnetization and the rotation about the coincident point, new magnetic parameters with a better stability-sensitivity ratio can be introduced in practice [9]. Figure 5(b) presents such a parameter, $\int_{-3\text{kA/m}}^{0} U_{env} dH$, which describes the evolution of the second negative-field peak of the BN envelope. The parameter has higher stability and sensitivity within the Lüders band region but only in the stress direction.

Our study of the magnetic anisotropy using the classical hysteresis method gives results similar to those recently published in reference [6]. The hysteresis loops, measured at different angles to the stress direction, rotate around the coincident points according to the simple formula $H(B, \varphi) = H(B, 0^o)\cos^2(\varphi) + H(B, 90^o)\sin^2(\varphi)$. The BN envelopes, measured at different angles, are shown in figure 6. Figure 7(a) presents the angle dependencies of the hysteresis coercive force for the differently strained samples. For the non-deformed sample, the results of measurement on one side with an expected slight anisotropy perpendicular to the rolling direction are shown.

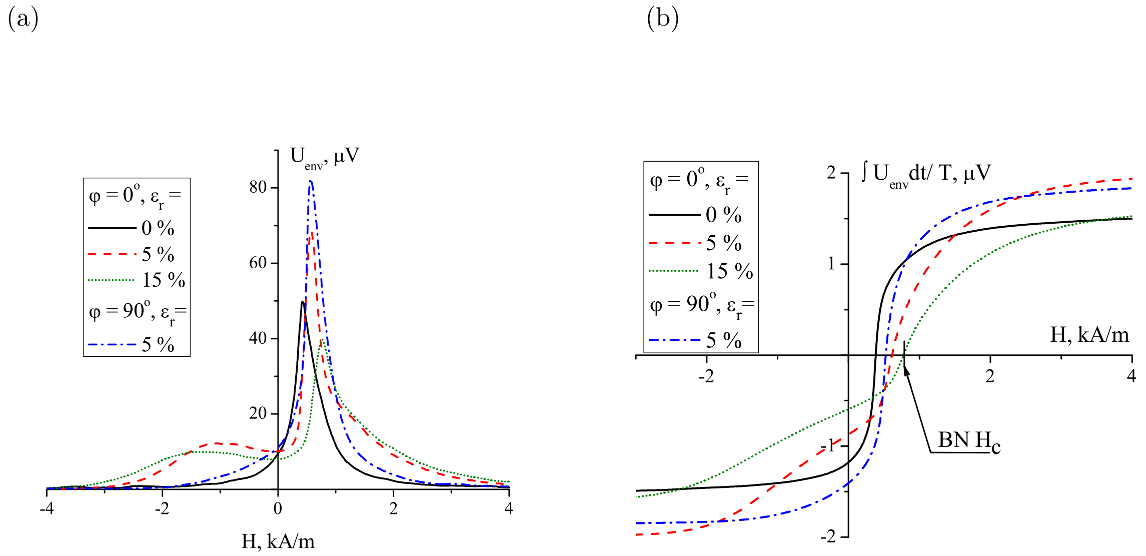

Figure 3. (a) BN envelopes for different residual strains and magnetization angles ($\varphi = 0^o$ is the stress direction). (b) The corresponding ascending branches of the BN loop normalized to the magnetization period T. The introduced BN coercive force, BN H_c, is denoted by the arrow.

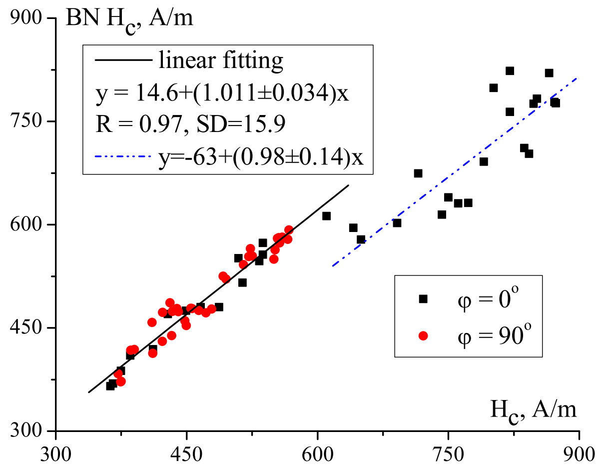

Figure 4. Correlation between the BN coercivity and the real coercive force. The Pearson correlation coefficient R and the standard deviation SD of the linear fit are given in the graph label.

Measurements on both sides are also presented separately for the sample, strained by $\sim$ 1% in the Lüders band region. As seen, there are different magnetic properties for $\varphi < 40^o$ along with different strain gauge readings of 2.05% and 0.037%. For these samples, the results are averaged over two symmetric angles $\pm\varphi$. For the two other specimens, strained beyond the Lüders band region, the data are additionally averaged over both sides. The error bars in figure 7 present the standard error of the averaging. All dependencies are well described by the proposed $\cos^2(\varphi)$ function [6, 8]. For the

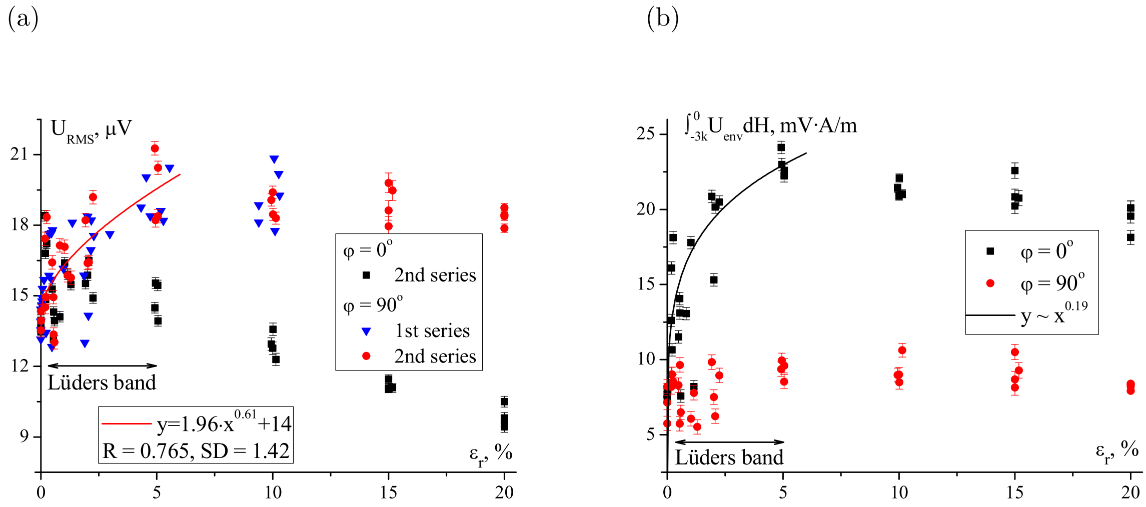

Figure 5. (a) RMS values of BN versus residual strain parallel and perpendicular to the stress ($\varphi = 0^{\rm o}$ is the stress direction). (b) Newly introduced parameter $\int_{-3{\rm kA/m}}^{0} U_{env} dH$ under the same conditions. The error bars present the standard error, estimated from the data deviation beyond the Lüders band region. For guidance, the dependencies within the Lüders band are fitted by a power law.

non-deformed and the 0.037% deformed samples, the freer $\cos^2(\varphi + \varphi_0)$ fitting is used. Figure 7(b) illustrates the angle dependencies of other basic magnetic parameters for the 10% strained sample: hysteresis loss $W = \oint HdB$, a newly introduced parameter $W_r = \int_0^{1.35} HdB$, the Barkhausen coercivity BN H_c, and the BN RMS value U_{RMS}. The normalized parameters are fitted by the $\cos^2(\varphi + \varphi_0)$ function. The former two hysteresis parameters, as for the hysteresis coercive force, are well described with zero φ_0. This is especially true for W_r, which is similar to the classical parameter $\int_{B_r}^{B_{max}} HdB$ in that it should represent the strain energy [2, 9]. However, contrary to the previously published statement [8, 11], the extremes of the BN parameters are found to deviate from the defined easy magnetization axis of $\varphi = 90^{\rm o}$ by $\varphi_0 = \pm 7 - 11^{\rm o}$: $\varphi_0 = 10.7^{\rm o}$ for BN H_c and $\varphi_0 = -7.9^{\rm o}$ for U_{RMS}.

4. Discussion

The ferromagnetic materials manifest an interesting and versatile magnetic response to mechanical deformation. We discuss each effect in turn, starting with the magnetic measurements *along the stress direction* for Fe-based steels with positive magnetostriction. *Applied tension* in the elastic range defines the easy magnetization axis and enhances magnetic properties owing to magnetoelastic coupling: the tension favours the 180° DWs, which are responsible for the remagnetization near coercivity [19]. On the other hand, the tension also disfavours the 90° DWs, which are necessary to close the intra-grain flux. The lack of 90° DWs reduces the DW mobility, leading to a subsequent degradation of the magnetic properties with higher stress (usually near the

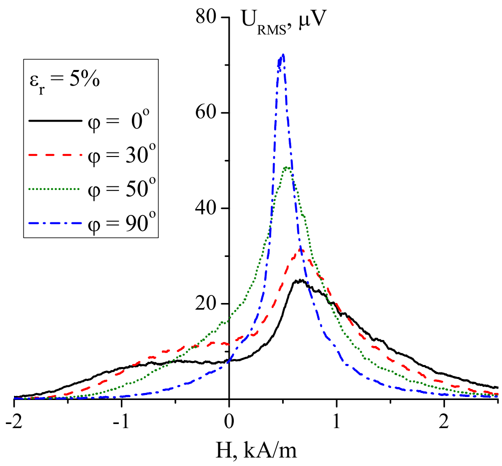

Figure 6. BN envelopes measured at different angles for the 5% strained sample ($\varphi = 0^o$ is the stress direction).

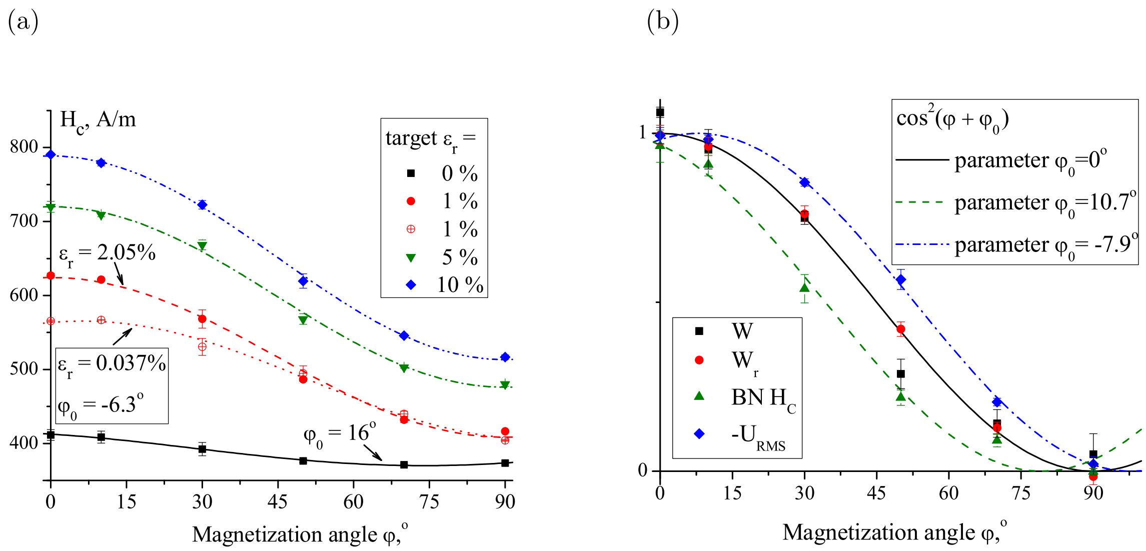

Figure 7. (a) Coercive force versus magnetization angle for the differently strained samples ($\varphi = 0^o$ is the stress direction). For the specimen, strained by $\sim 1\%$ in the Lüders band region, the measurements made on the opposite sample sides are presented separately (● and ○ symbols). (b) Other normalized magnetic parameters versus magnetization angle for the 10% strained sample: hysteresis loss $W = \oint HdB$, an introduced parameter $W_r = \int_0^{1.35} HdB$, the Barkhausen coercivity BN H_c, and the BN RMS value U_{RMS}. For both graphs, the results are averaged over two symmetrical angles $\pm\varphi$ and both sample sides. For the fitting the $\cos^2(\varphi + \varphi_0)$ function is used. The error bars present the standard error of the averaging.

yield point) [20]. With plastic tension, the accumulated dislocations additionally hinder DW motion, leading to further magnetic degradation [7].

After unloading from tension, the magnetic properties dramatically deteriorate and the remagnetization has two distinguishable phases (see figure 3(a)). The second peak of the differential permeability and that of the BN envelope at negative fields are ascribed to the 90° DW activity, favoured by the compressive residual stress [3, 5, 6]. The formed dislocation pattern splits the initial $\sim 10\ \mu$m ferrite grains into several micron compressed regions, as shown by transmission electron microscopy and X-ray and neutron diffraction measurements [7, 12, 21, 22]. Because of the complexity of the BN response, there is a higher signal at low strain, where DWs can still jump over the single dislocations (see figure 5(a)) [4, 7, 10]. With higher strain, the dislocation tangles form a closed pattern, which deteriorates the magnetic properties similarly to a decrease in grain size [18, 23].

Applied compression results in the same two-peak remagnetization and degradation of the magnetic properties, which proves the hypothesis of the magnetoelastic coupling with the 90° DWs [17, 23]. Moreover, the magnetoacoustic emission, which is sensitive to the 90° DW motion only, has stronger response under compression than under tension [24]. *After unloading* from compression, the magnetic properties are enhanced because of residual tensile stress; the remagnetization occurs in a usual one-peak manner [22, 23].

The interesting issue of magnetic anisotropy caused by uniaxial deformation has been scarcely investigated so far. The $\mathrm{BN_{energy}}(\varphi)$ parameter (maximum of the BN loop), which usually behaves similarly to the RMS value U_{RMS}, was evaluated for applied tension and compression [4, 8]. The hysteresis of plastically stretched steel after unloading was studied in detail only recently [6]. The first comprehensive BN investigation of the problem is presented in this work (see figures 3-6 and 7(b)). Our measurements proved that the easy magnetization axis aligns perpendicular to the compressive residual stresses in the deformation direction (see figure 7) [12, 21]. Along the axis of easy magnetization, none of the magnetic parameters except the RMS value of BN change considerably with strain (see figures 2(b) and 5). The angle dependencies of the classical magnetic parameters are well fitted by the $\cos^2$ function, proving their relation with the strain energy in its simplest form $E_\sigma = 3/2\lambda_s\sigma\sin^2(\varphi + 90^\circ)$ [2]. For the BN parameters, however, there is a $\sim 10^\circ$ shift of their extremes from the easy magnetization axis owing to more complex coupling of the BN signal with the steel microstructure (see figure 7(b)) [10]. Therefore, the current approach for determination of the easy magnetization axis using the BN technique should be revised [4, 8]. In addition, it is worth noting that the two-peak magnetization behaviour seems to be typical for any magnetization perpendicular to the easy magnetization axis [6].

Another special problem is the magnetic response in the Lüders band region, which has also been little studied [9, 11, 19]. In this region of plastic instability two dislocation bands gradually spread from the sample ends through the specimen bulk. This leads to localized regions of plastic deformation and substantial variations in our measurement results (see figures 2(b), 5 and 7(a)) [12]. Our data additionally indicated that in the Lüder region the magnetic response could show small tensile residual stress along the deformation direction and compressive residual stress in the perpendicular direction. With the formation of a stable dislocation-stress pattern beyond the Lüders band region, our results also become stable. In contrast to our expectations, the bulk hysteresis and the local BN measurements have the same response in the Lüders band region (see figure 4). The previously observed difference at higher strains for the deformation direction is probably due to degradation of the sample surface that is heavier than that of its bulk [10].

The magnetic response to the mechanical deformation is substantially dependent on the material microstructure. The presented behaviour is typical for low-carbon steels with dominant fraction of the ferrite phase [1, 2, 3, 4, 6]. Iron single-crystal does not show the two-peak magnetization because of the lack of 90° DWs. However, pure polycrystalline iron and ferritic steels do manifest this behaviour – the 90° DWs occupy the grain boundaries [5, 19, 25]. Therefore, it can be assumed that similar magnetic properties of the SS400 steel is mostly determined by the DW motion inside the ferrite grains. However, second order residual stresses between the ferrite and the pearlite constituents can influence the magnetic response [26]. Additional investigations of the steels with different pearlite fraction are necessary to establish the quantitative correlations between the magnetic parameters and the 2nd order residual stress. Qualitative trend is known from the literature: for harder steels, the considered magnetic features gradually disappear. Higher internal stresses make the magnetic properties of the hard steels almost independent of the applied external deformations [21, 23, 27]. Ni-based alloys with negative magnetostriction have the opposite response to mechanical stresses, which demonstrates the importance of magnetoelastic coupling in explaining the considered phenomena [2, 17].

This work also displays the potential of magnetic methods for the non-destructive testing of plastic deformation. Our industrial partner needs a reliable technique to distinguish between the non-deformed and the plastically deformed steel states. The sensitivity of the shown magnetic parameters is high and prevailed over the measurement error in the region of small plastic strains – so the methods are potentially applicable for this industrial task. However, most of the magnetic parameters are sensitive only in the deformation direction (see figures 2(b) and 5(b)) [7, 9]. Therefore, the different strain dependencies of the RMS value of BN are worthy of note. This parameter can be solely used for detection of small plastic strains in the direction perpendicular to the deformation (see figure 5(a)).

However, special attention should be paid to the problem of repeatability of the measurements. Good result statistics make the analysis of the measurement uncertainties possible. In this work the measurement uncertainty is estimated as the random error of series of identical observations – the error bars of figures 2(b), 5, and 7 present the standard measurement error. The obtained standard errors are about 2-3% of the measured values, which is a quite satisfactory mistake level [28]. It depends on many uncontrollable experimental factors: the yoke-sample and the BN coil lift-offs, mistakes of the Hall array calibration and its angle positioning, etc [15]. It should be also taken into account that this mistake additionally includes the technological deviations of steel microstructure, which can provide the comparable result deviations [29]. We neglect the systematic error of our laboratory devices, which maximum level is expected to be about 0.5-1%. To improve the measurement technique repeatability at industrially relevant magnetization frequencies, an iterative digital feedback procedure is being developed to control the magnetic field/flux waveform [14, 15].

5. Conclusions

This work presents a comprehensive investigation of the influence of plastic deformation on the magnetic properties of structural low-carbon steel. The bulk hysteresis and the local BN methods demonstrate similar responses. The nonhomogeneity of the dislocation-stress pattern within the Lüders band region leads to the scattering of values for magnetic parameters, which stabilizes at higher strains. Most parameters have highest sensitivity to the residual strain along the deformation direction (hard magnetization axis). Only the RMS value of BN has a sharp monotonic increase in the perpendicular direction (easy magnetization axis). The induced magnetic anisotropy is well described by the simple $\cos^2$ law. The extremes of the BN parameters shift $\pm 10^{o}$ from the real easy magnetization axis. The residual compressive stresses are shown to be the main driving force of the observed magnetic behaviour with several interesting features.

Acknowledgments

We would like to express our thanks to Tokyo Electric Power Company for the sample preparation and the publishing permission. O. Stupakov appreciates the financial support of the Japanese Society for Promotion of Science (JSPS) under the postdoctoral fellowship program and that of the Czech Science Foundation (GACR) under postdoctoral project No. 102/09/P108. The work was also supported by the Academy of Sciences of the Czech Republic under the project AVOZ10100520. The authors are very thankful to Prof. J. Bydžovský and Dr. J. Pal'a for their careful reading of the manuscript and many helpful remarks, and to Dr. A. Jäger and Prof. B. Skrbek for their assistance with optical microstructure analysis.

References

[1] Ewing J A 1892 *Magnetic Induction in Iron and Other Metals* (London: The Electrician) ch IX
[2] Bozorth R M 2003 *Ferromagnetism* (New York: IEEE Press) ch 13
[3] Stefanita C G, Atherton D L and Clapham L 2000 Plastic versus elastic deformation effects on magnetic Barkhausen noise in steel *Acta Mater.* **48** 3545–51

[4] Dhar A, Clapham L and Atherton D L 2001 Influence of uniaxial plastic deformation on magnetic Barkhausen noise in steel *NDT&E Int.* **34** 507–14
[5] Stupakov O, Pala J, Tomáš I, Bydžovský J and Novák V 2007 Investigation of magnetic response to plastic deformation of low-carbon steel *Mater. Sci. Eng.* A **462** 351-4
[6] Perevertov O 2007 Influence of the residual stress on the magnetization process in mild steel *J. Phys. D: Appl. Phys.* **40** 949–54
[7] Pala J, Stupakov O, Bydžovský J, Tomáš I and Novák V 2007 Magnetic behaviour of low-carbon steel in parallel and perpendicular directions to tensile deformation *J. Magn. Magn. Mater.* **310** 57–62
[8] Krause T W, Clapham L, Pattantyus A and Atherton D L 1996 Investigation of the stress-dependent magnetic easy axis in steel using Barkhausen noise *J. Appl. Phys.* **79** 4242–52
[9] Stupakov O and Tomáš I 2006 Hysteresis minor loop analysis of plastically deformed low-carbon steel *NDT&E Int.* **39** 554–61
[10] Stupakov O, Pala J, Yurchenko V, Tomáš I and Bydžovský J 2008 Measurement of Barkhausen noise and its correlation with magnetic permeability *J. Magn. Magn. Mater.* **320** 204–9
[11] Dhar A, Clapham L and Atherton D L 2002 Influence of Lüders bands on magnetic Barkhausen noise and magnetic flux leakage signals *J. Mater. Sci.* **37** 2441–6
[12] Hutanu R, Clapham L and Rogge R B 2005 Intergranular strain and texure in steel Luders bands *Acta Mater.* **53** 3517–24
[13] Stupakov O, Tomáš I, Pal'a J, Bydžovský J, Bošanský J and Šmida T 2004 Traditional, Barkhausen and MAT magnetic response to plastic deformation of low-carbon steel *Czech. J. Phys.* **54** D47–50
[14] Stupakov O, Kikuchi H, Liu T and Takagi T 2009 Applicability of local magnetic measurements *Measurement* **42** 706-10
[15] Stupakov O, Pal'a J, Takagi T and Uchimoto T 2009 Governing conditions of repeatable Barkhausen noise response *J. Magn. Magn. Mater.* **321** 2956–62
[16] Stupakov O, Tomáš I and Kadlecová J 2006 Optimization of single-yoke magnetic testing by surface fields measurement *J. Phys. D: Appl. Phys.* **39** 248–54
[17] Bulte D P and Langman R A 2002 Origin of the magnetomechanical effect *J. Magn. Magn. Mater.* **251** 229–43
[18] Sablik M J, Rios S, Landgraf F J G, Yonamine T and Campos M F 2005 Modelling of sharp change in magnetic hysteresis behavior of electrical steel at small plastic deformation *J. Appl. Phys.* **97** 10E518
[19] Stupakov O 2006 *Investigation of Magnetic Processes of Structure-degraded Ferromagnetic Materials* (Charles University in Prague: Doctoral thesis) ch 2. Available from: www.fzu.cz/~stupak/Thesis.pdf
[20] Shilling J W and Houze G L 1974 Magnetic properties and domain structure in grain-oriented 3% Si-Fe *IEEE Trans. Magn.* **MAG-10** 195–223
[21] Oliver E C, Daymond M R and Withers P J 2004 Interphase and intergranular stress generation in carbon steels *Acta Mater.* **52** 1937–51
[22] Cullity B D 1964 Sources of error in X-ray measurements of residual stress *J. Appl. Phys.* **35** 1915–7
[23] Gatelier-Rothea C, Chicois J, Fougeres R and Fleischmann P 1998 Characterization of pure iron and carbon-iron binary alloy by Barkhausen noise measurements: study of the influence of stress and microstructure *Acta Mater.* **46** 4873–82
[24] Kusanagi H, Kimura H and Sasaki H 1979 Stress effect on the magnitude of acoustic emission during magnetization of ferromagnetic materials *J. Appl. Phys.* **50** 2985–7
[25] Takahashi S, Echigoya J and Motoki Z 2000 Magnetization curves of plastically deformed Fe metals and alloys *J. Appl. Phys.* **87** 805–13
[26] Altpeter I, Dobmann G, Kröning M, Rabung M and Szielasko S 2009 Micro-magnetic evaluation of micro residual stresses of the IInd and IIInd order *NDT&E Int.* **42** 283–90

[27] Jiles D C 1988 The effect of compressive plastic deformation on the magnetic properties of AISI 4130 steels with various microstructures *J. Phys. D: Appl. Phys.* **21** 1196–204

[28] Stupakov O, Wood R, Melikhov Y and Jiles D 2010 Measurement of electrical steels with direct field determination *IEEE Trans. Magn.* **46** 298–301

[29] Korzunin G S, Chistyakov V K and Rimshev F F 2001 Developing techniques for testing magnetic properties of electric steels. II. Variations in magnetic properties and their effect on reliability of testing results (review article) *Russ. J. Nondestr. Test.* **37** 239–62